Simplified Soft-Output Detection of CPM Signals Over Coherent and Phase Noise Channels

Alan Barbieri and Giulio Colavolpe, *Member, IEEE*

***Abstract*— We consider continuous phase modulations (CPMs) in iteratively decoded serially concatenated schemes. Although the overall receiver complexity mainly depends on that of the CPM detector, almost all papers in the literature consider the optimal maximum a posteriori (MAP) *symbol* detection algorithm and only a few attempts have been made to design low-complexity suboptimal schemes. This problem is faced in this paper by first considering the case of an ideal coherent detection, then extending it to the more interesting case of a transmission over a typical satellite channel affected by phase noise. In both cases, we adopt a simplified representation of an M-ary CPM signal based on the principal pulses of its Laurent decomposition. Since it is not possible to derive the exact detection rule by means of a probabilistic reasoning, the framework of factor graphs (FGs) and the sum-product algorithm (SPA) is used. In the case of channels affected by phase noise, continuous random variables representing the phase samples are explicitly introduced in the FG. By pursuing the principal approach to manage continuous random variables in a FG, i.e., the canonical distribution approach, two algorithms are derived which do not require the presence of known (pilot) symbols, thanks to the intrinsic differential encoder embedded in the CPM modulator.**

***Index Terms*— Factor graphs, sum-product algorithm, continuous phase modulation, iterative detection and decoding, detection and decoding in the presence of phase noise.**

I. Introduction

CONTINUOUS phase modulations (CPMs) form a class of constant envelope signaling formats that are efficient in power and bandwidth [1]. Moreover, the recursive nature of the modulator makes the CPM signaling formats attractive in serially concatenated schemes to be iteratively decoded [2], [3].

Several decomposition approaches for CPM signals, applied to the design of detection algorithms, were presented in the literature. For serially concatenated CPM signals with iterative decoding, the Rimoldi decomposition approach [4] is usually adopted to derive the optimal maximum a posteriori (MAP) *symbol* detection algorithm (e.g., see [3], [5]). However, for this approach an explicit technique for state reduction, such as that in [6], must be employed to limit the receiver complexity [7]. A similar observation can be made for other approaches based on alternative representations of a CPM signal, such as those in [8]–[10].

On the contrary, the Laurent representation, originally devised in [11] for binary modulation formats and extended to the general case of M-ary CPM signals in [12], is more attractive from the point of view of the receiver complexity reduction. This representation allows to decompose a CPM signal as a superposition of linearly modulated signals. The observation that most of the signal power is contained in a limited number of linearly modulated components (the so-called $M-1$ *principal components*) allows to design a receiver based on these components only, simplifying the receiver front-end and automatically reducing the number of trellis states, at least if MAP *sequence* detection and the Ungerboeck observation model are adopted, as in [13].[1] In fact, for the Forney observation model, a more complex multidimensional whitened matched filter (WMF) must be adopted [15], and it can be also shown that the "automatic" state reduction does not happen, due to the memory introduced by the WMF.

The generalization of the approach in [13] to MAP *symbol* detection of CPM signals, although in a perfectly coherent setting, is not trivial. All the well known materializations of the MAP *symbol* detection strategy in the literature (e.g., see [17]) have been obtained by using a probabilistic derivation based on the chain rule and the properties of a Markov source observed through a discrete memoryless channel. Hence, this derivation cannot be directly extended to the Ungerboeck observation model. For linear modulations in the presence of intersymbol interference, this problem has been recently solved in [18] by using a properly defined factor graph (FG) and the sum-product algorithm (SPA) [19]. In this paper, this solution will be extended to CPM signals by first considering the case of ideal coherent detection. It will be shown that the designed reduced-complexity detection algorithms entail only a minor performance degradation with respect to the optimal MAP *symbol* detectors when employed in serially concatenated schemes with iterative detection/decoding.

We will then consider the more interesting case of a transmission over a typical satellite channel affected by phase noise. Although several soft-input soft-output (SISO) detection algorithms suitable for iterative detection/decoding have been

Paper received November 1, 2005, revised June 1, 2006 and October 31, 2006; accepted February 16, 2007. The associate editor coordinating the review of this paper and approving it for publication was J. Tugnait. This paper was presented in part at the International Symposium on Information Theory and its Applications (ISITA'04), Parma, Italy, October 2004, at the IEEE Global Telecommunications Conference (GLOBECOM'05), St. Louis, MO, U.S.A., November-December 2005, and at the 14th European Signal Processing Conference (EUSIPCO'06), Florence, Italy, September 2006. This work is funded by the European Space Agency, ESA-ESTEC, Noordwijk, The Netherlands, under contract no. 19370/05/NL/JD.

The authors are with the Università di Parma, Dipartimento di Ingegneria dell'Informazione, Parco Area delle Scienze 181A, I-43100 Parma, Italy (e-mail: barbieri@tlc.unipr.it, giulio@unipr.it).

Digital Object Identifier 10.1109/TWC.2007.05872.

[1] In analogy with the problem of detection in the presence of intersymbol interference, for CPM signals a set of sufficient statistics obtained through a bank of filters matched to the pulses of the Laurent representation, as in [13], is said to form the Ungerboeck observation model [14]. On the contrary, when the multidimensional whitened matched filter front-end described in [15] is used, we say that the Forney observation model is employed for detection [16].

recently designed for linear modulations transmitted over channels affected by a time-varying phase (see for example [20]–[22] and references therein), less attention has been devoted to CPM signals. An exception is represented by [23], [24] where, based on the approach in [21], [25], joint detection and phase synchronization is performed by working on the trellis of the CPM signal or on an expanded trellis and using *multiple* phase estimators in a per-survivor fashion.[2] In this paper, we adopt a Bayesian approach, i.e., the channel phase is modeled as a stochastic process with known statistics. In particular, we model the phase noise as a Wiener process. By still using the FG/SPA framework, we derive the exact MAP *symbol* detection strategy under the above mentioned simplified representation of a CPM signal as sum of the principal pulses of its Laurent decomposition. We analyze the properties of this detection strategy finding that it can be implemented by using a *single* forward-backward estimator of the phase probability density function, followed by a symbol-by-symbol completion to produce the a posteriori probabilities (APPs) of the information symbols. Then, by using the canonical distribution approach [26], we develop a couple of practical schemes with different complexity to implement the forward-backward estimator. The resulting algorithms obviously work in a joint demodulation/phase tracking fashion, do not require the insertion of pilot symbols, and may be used as SISO blocks for iterative detection/decoding in concatenated schemes.

The remainder of this paper is organized as follows. In Section II, we provide the signal model and briefly review the Laurent decomposition. By means of the FG/SPA framework, a low-complexity MAP symbol detection algorithm is derived in Section III for the coherent channel, and extended to the phase noise channel in Section IV. The performance of the proposed receivers is assessed in Section V. Finally, some conclusions are drawn in Section VI.

II. Signal Model and Laurent Decomposition

The complex envelope of a CPM signal has the form [1]

$$s(t,\boldsymbol{\alpha}) = \sqrt{\frac{2E_S}{T}}\,\exp\{j2\pi h \sum_{n=0}^{N-1} \alpha_n q(t-nT)\} \qquad (1)$$

in which E_S is the energy per information symbol, T is the symbol interval, $h = r/p$ is the modulation index (r and p are relatively prime integers), the information symbols $\{\alpha_n\}$ are assumed independent and take on values in the M-ary alphabet $\{\pm 1, \pm 3, \ldots, \pm(M-1)\}$, $\boldsymbol{\alpha} = \{\alpha_n\}$ denotes the information sequence, and finally N is the number of transmitted information symbols. The function $q(t)$ is the *phase-smoothing response* and its derivative is the *frequency pulse*, assumed of duration LT.

Based on Laurent representation, the complex envelope of a CPM signal may be exactly expressed as [12]

$$s(t,\boldsymbol{\alpha}) = \sum_{k=0}^{Q^{\log_2 M}(M-1)-1} \sum_{n} a_{k,n} p_k(t-nT) \qquad (2)$$

in which M is assumed to be a power of two to simplify the notation, $Q \triangleq 2^{L-1}$, and the expressions of pulses $\{p_k(t)\}$ and those of symbols $\{a_{k,n}\}$ as a function of the information symbol sequence $\{\alpha_n\}$ may be found in [12] (see this reference for the general case of M non-power of two). By truncating the summation in (3) considering only the first $K < Q^{\log_2 M}(M-1)$ terms, we obtain an approximation of $s(t,\boldsymbol{\alpha})$:

$$s(t,\boldsymbol{\alpha}) \simeq \sum_{k=0}^{K-1} \sum_{n} a_{k,n} p_k(t-nT)\,. \qquad (3)$$

Most of the signal power is concentrated in the first $M-1$ components, i.e., those associated with the pulses $\{p_k(t)\}$ with $0 \le k \le M-2$, which are denoted as *principal components* [12]. As a consequence, a value of $K = M-1$ may be used in (3) to attain a very good tradeoff between approximation quality and number of signal components and in fact, it was shown in [13] that MAP *sequence* detection receivers only based on principal pulses practically attain the performance of the corresponding optimal detector. A nice feature of the principal components is that their symbols $\{a_{k,n}\}_{k=0}^{M-2}$ can be expressed as a function of the information symbol α_n and of symbol $a_{0,n-1}$, only [12]. As an example, symbol $a_{0,n}$ can be computed as [12]

$$a_{0,n} = a_{0,n-1} e^{j\pi h \alpha_n}\,. \qquad (4)$$

In Section III, the case of an ideal coherent channel will be analyzed. Hence, in that section $a_{0,-1}$ will be assumed known to the receiver. On the contrary, since in Section IV the transmission over a channel affected by phase noise will be considered, we will assume that the initial symbol $a_{0,-1}$ is unknown to the receiver due to the initial channel phase uncertainty. Symbols $\{a_{0,n}\}$ take on p values [12]. They belong to the alphabet $\mathcal{A}_o = \{e^{j2\pi hm}, m = 0,1,\ldots,p-1\}$ when n is odd, or to the alphabet $\mathcal{A}_e = \{e^{j\pi h} e^{j2\pi hm}, m = 0,1,\ldots,p-1\}$ when n is even.[3]

We employ the following equivalent representation for symbols α_n and $a_{0,n}$ [4]:

$$\alpha_n = 2\bar{\alpha}_n - (M-1) \qquad (5)$$

$$a_{0,n} = e^{-j\pi h(M-1)(n+1)} e^{j2\pi h\phi_n} \qquad (6)$$

where $\bar{\alpha}_n \in \{0,1,\ldots,M-1\}$, $\phi_n \in \{0,1,\ldots,p-1\}$. The integer ϕ_n can be recursively updated as

$$\phi_n = [\phi_{n-1} + \bar{\alpha}_n]_p \qquad (7)$$

where $[\cdot]_p$ denotes the "modulo p" operator. In this way we have defined a one-to-one correspondence between sequences $\{a_{0,n}\}$ and $\{\phi_n\}$.

III. MAP Symbol Detection on a Coherent Channel

In [13], simplified MAP *sequence* detectors based on the Viterbi algorithm have been designed for the ideal coherent channel. In this case, the approximate representation of an M-ary CPM signal based on the principal pulses of its Laurent

[2] As a particular case of this general approach, the use of a single phase estimator is also considered in [24] to trade performance for complexity.

[3] When r is even, $\mathcal{A}_o$ and $\mathcal{A}_e$ coincide.

decomposition plays a major role. In fact, starting from the complex envelope of the received signal

$$r(t) = s(t, \boldsymbol{\alpha}) + w(t) \tag{8}$$

where $w(t)$ is a complex-valued additive white Gaussian noise (AWGN) process with independent components, each with two-sided power spectral density N_0, representing the received signal onto an orthonormal basis and denoting by $\mathbf{r}$ its vector representation, exploiting the constant envelope property of a CPM signal, it is found that [13][4]

$$p(\mathbf{r}|\boldsymbol{\alpha}) = p(\mathbf{r}|\boldsymbol{\alpha}, \boldsymbol{\phi}) \mathrel{\tilde{\propto}} \prod_n G_n(\alpha_n, \phi_{n-1}) \tag{9}$$

where $\boldsymbol{\phi} = \{\phi_n\}$ and

$$G_n(\alpha_n, \phi_{n-1}) = \exp\left\{\frac{1}{N_0}\mathrm{Re}\left[\sum_{k=0}^{M-2} x_{k,n} a_{k,n}^*\right]\right\} \tag{10}$$

and $x_{k,n} = r(t) \otimes p_k(-t)|_{t=nT}$ is the output, at discrete-time nT of a filter matched to the pulse $p_k(t)$. Symbol $\mathrel{\tilde{\propto}}$ has been used to denote an approximate proportionality relationship. The approximation here is related to the fact that we are considering the principal components only. Notice that the functions $G_n(\alpha_n, \phi_{n-1})$ are not probability density functions (pdfs) nor they are proportional to pdfs. In the arguments of G_n, we omitted the explicit dependence on the received signal since this latter is known to the receiver, and exploited the above mentioned property that all symbols $\{a_{k,n}\}_{k=0}^{M-2}$ in (10) depend on α_n and ϕ_{n-1} only. In order to implement the MAP *sequence* detection strategy, the maximization of the pdf $p(\mathbf{r}|\boldsymbol{\alpha})$ can be performed by using the Viterbi algorithm with branch metrics given by $\ln G_n(\alpha_n, \phi_{n-1}) \propto \mathrm{Re}[\sum_{k=0}^{M-2} x_{k,n} a_{k,n}^*]$. Hence, the resulting receiver works on a trellis whose state is defined by ϕ_{n-1}, and thus the number of trellis states is p [13].

We now extend this technique for complexity reduction to MAP *symbol* detection. The joint a posteriori probability mass function (pmf) $P(\boldsymbol{\alpha}, \boldsymbol{\phi}|\mathbf{r})$ can be expressed as

$$P(\boldsymbol{\alpha}, \boldsymbol{\phi}|\mathbf{r}) \propto P(\boldsymbol{\phi}|\boldsymbol{\alpha}) P(\boldsymbol{\alpha}) p(\mathbf{r}|\boldsymbol{\alpha}, \boldsymbol{\phi}) \,. \tag{11}$$

By using (9) and observing that we can further factor the terms $P(\boldsymbol{\alpha})$ and $P(\boldsymbol{\phi}|\boldsymbol{\alpha})$ in (11) as

$$P(\boldsymbol{\alpha}) = \prod_{n=0}^{N-1} P(\alpha_n) \tag{12}$$

$$P(\boldsymbol{\phi}|\boldsymbol{\alpha}) = P(\phi_{-1}) \prod_{n=0}^{N-1} I_n(\phi_n, \phi_{n-1}, \alpha_n) \tag{13}$$

where $I_n(\phi_n, \phi_{n-1}, \alpha_n)$ is an indicator function, equal to 1 if α_n and states ϕ_{n-1} and ϕ_n respect the constraint (7), and to zero otherwise, we obtain

$$P(\boldsymbol{\alpha}, \boldsymbol{\phi}|\mathbf{r}) \mathrel{\tilde{\propto}} P(\phi_{-1}) \prod_{n=0}^{N-1} I_n(\phi_n, \phi_{n-1}, \alpha_n) \cdot P(\alpha_n) G_n(\alpha_n, \phi_{n-1}) \,. \tag{14}$$

[4]In [13] the reader will not find the expression of $p(\mathbf{r}|\boldsymbol{\alpha})$ but of the likelihood function which is proportional to $\ln p(\mathbf{r}|\boldsymbol{\alpha})$.

The corresponding FG is depicted in Fig. 1 and we can observe that it is cycle-free. Hence, the application to it of the SPA with a *non-iterative* forward-backward schedule, produces the *exact* marginal APPs of symbols $\{\alpha_n\}$ (except for the approximation related to the use of the principal components only). In the figure, we defined $P_e(\alpha_n)$ as the extrinsic APP of α_n, i.e., $P_e(\alpha_n) = P(\alpha_n|\mathbf{r})/P(\alpha_n)$. With reference to the messages in the figure, by applying the updating rules of the SPA, messages $\mu_{f,n}(\phi_n)$ and $\mu_{b,n}(\phi_n)$ can be recursively computed by means of the following forward and backward recursions:

$$\begin{aligned}\mu_{f,n}(\phi_n) &= \sum_{\phi_{n-1}} \sum_{\alpha_n} \mu_{f,n-1}(\phi_{n-1}) G_n(\alpha_n, \phi_{n-1}) \\ &\quad \cdot I_n(\phi_n, \phi_{n-1}, \alpha_n) P(\alpha_n) \qquad (15) \\ &= \sum_{\alpha_n} \mu_{f,n-1}(\check{\phi}_{n-1}) G_n(\alpha_n, \check{\phi}_{n-1}) P(\alpha_n)\end{aligned}$$

$$\begin{aligned}\mu_{b,n-1}(\phi_{n-1}) &= \sum_{\phi_n} \sum_{\alpha_n} \mu_{b,n}(\phi_n) G_n(\alpha_n, \phi_{n-1}) \\ &\quad \cdot I_n(\phi_n, \phi_{n-1}, \alpha_n) P(\alpha_n) \qquad (16) \\ &= \sum_{\alpha_n} \mu_{b,n}(\hat{\phi}_n) G_n(\alpha_n, \phi_{n-1}) P(\alpha_n)\end{aligned}$$

where in (15) $\check{\phi}_{n-1} = [\phi_n - \bar{\alpha}_n]_p$ (i.e., given ϕ_n and α_n, $\check{\phi}_{n-1}$ is such that $I_n(\phi_n, \check{\phi}_{n-1}, \alpha_n) = 1$), whereas in (16) $\hat{\phi}_n = [\phi_{n-1} + \bar{\alpha}_n]_p$ (i.e., given ϕ_{n-1} and α_n, $\hat{\phi}_n$ is such that $I_n(\hat{\phi}_n, \phi_{n-1}, \alpha_n) = 1$), and with the following initial conditions:

$$\mu_{f,-1}(\phi_{-1}) = P(\phi_{-1}) \tag{17}$$

$$\mu_{b,N-1}(\phi_{N-1}) = 1/p \,. \tag{18}$$

Finally, the extrinsic APPs of symbols $\{\alpha_n\}$ can be computed by means of the following completion

$$\begin{aligned}P_e(\alpha_n) &= \sum_{\phi_{n-1}} \sum_{\phi_n} \mu_{f,n-1}(\phi_{n-1}) \mu_{b,n}(\phi_n) \\ &\quad \cdot I_n(\phi_n, \phi_{n-1}, \alpha_n) G_n(\alpha_n, \phi_{n-1}) \qquad (19) \\ &= \sum_{\phi_n} \mu_{f,n-1}(\check{\phi}_{n-1}) \mu_{b,n}(\phi_n) G_n(\alpha_n, \check{\phi}_{n-1}) \,.\end{aligned}$$

Roughly speaking, the complexity is reduced by a factor given by $p/(pM^{L-1})$, that is the ratio between the receiver states of the reduced-complexity and optimal schemes.

IV. MAP Symbol Detection on a Phase Noise Channel

We now consider the transmission of a CPM signal over a typical satellite channel affected by phase noise. In this case, the complex envelope of the received signal can be modeled as

$$r(t) = s(t, \boldsymbol{\alpha}) e^{j\theta(t)} + w(t) \tag{20}$$

where $\theta(t)$ is the phase noise introduced by the channel. We model the phase noise $\theta(t)$ as a time-continuous Wiener process [27], [28] with incremental variance over a signaling interval equal to σ_Δ^2. The assumption on the phase noise model will be relaxed in the numerical results. We also assume that the channel phase $\theta(t)$ is slowly varying such that it can be

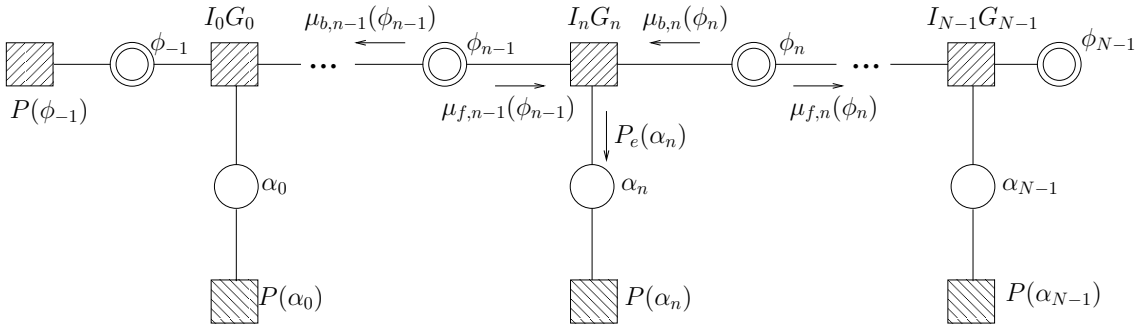

Fig. 1. Factor graph corresponding to eqn. (14).

considered constant over the duration of the pulses $\{p_k(t)\}$. In other words we assume that

$$\int_{-\infty}^{+\infty} r(t)p_k(t-nT)e^{-j\theta(t)}\,dt = e^{-j\theta_n}\int_{-\infty}^{+\infty} r(t)p_k(t-nT)e^{j[\theta_n-\theta(t)]}\,dt \simeq e^{-j\theta_n}\int_{-\infty}^{+\infty} r(t)p_k(t-nT)\,dt = e^{-j\theta_n}x_{k,n} \quad (21)$$

having defined $\theta_n = \theta(nT)$ and assumed $\theta_n - \theta(t) \simeq 0$ where $p_k(t-nT) \neq 0$, for the slowly varying assumption. Hence, under this hypothesis, the output, sampled at the symbol rate, of a bank of filters matched to the pulses $\{p_k(t)\}$ is still a set of sufficient statistics for this detection problem. As in the previous section, we use a simplified set represented by the output of a bank of filters matched to the principal pulses $\{p_k(t)\}_{k=0}^{M-2}$. From (21), only the samples of $\theta(t)$ at discrete-time nT are significant. These samples satisfy the discrete-time Wiener model:

$$\theta_{n+1} = \theta_n + \Delta_n \quad (22)$$

where $\{\Delta_n\}$ are real independent and identically distributed Gaussian random variables with zero mean and standard deviation σ_Δ,[5] and θ_0 is assumed uniformly distributed in $[0, 2\pi)$.

We now derive the MAP *symbol* detection strategy for this case. To this purpose, we first compute the joint distribution[6] $p(\boldsymbol{\alpha}, \boldsymbol{\phi}, \boldsymbol{\theta}|\mathbf{r})$, where $\boldsymbol{\theta} = \{\theta_n\}$. Its expression is

$$p(\boldsymbol{\alpha}, \boldsymbol{\phi}, \boldsymbol{\theta}|\mathbf{r}) \propto P(\boldsymbol{\phi}|\boldsymbol{\alpha})P(\boldsymbol{\alpha})p(\boldsymbol{\theta})p(\mathbf{r}|\boldsymbol{\alpha}, \boldsymbol{\theta}, \boldsymbol{\phi})\,. \quad (23)$$

We can now express [13]

$$p(\mathbf{r}|\boldsymbol{\alpha}, \boldsymbol{\theta}, \boldsymbol{\phi}) \,\widetilde{\propto}\, \prod_n H_n(\alpha_n, \phi_{n-1}, \theta_n) \quad (24)$$

having defined, in this case,

$$H_n(\alpha_n, \phi_{n-1}, \theta_n) = \exp\left\{\frac{1}{N_0}\mathrm{Re}\left[e^{-j\theta_n}\sum_{k=0}^{M-2} x_{k,n}a_{k,n}^*\right]\right\}. \quad (25)$$

[5]Note that, since the channel phase is defined modulo 2π, the probability density function (pdf) $p(\theta_{n+1}|\theta_n)$ can be approximated as Gaussian only if $\sigma_\Delta \ll 2\pi$.

[6]We still use the symbol $p(.)$ to denote a continuous pdf with some discrete probability masses.

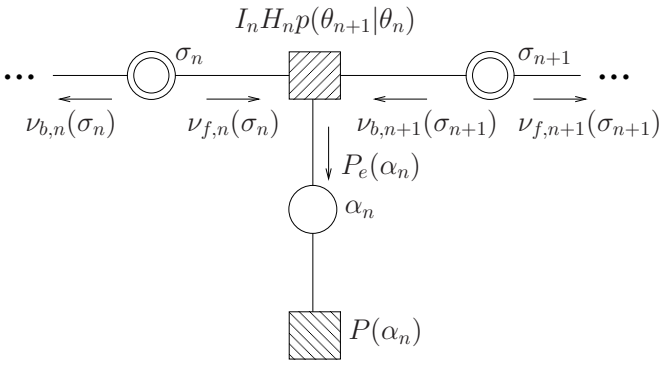

Fig. 2. Factor graph corresponding to eqn. (27).

By using (12) and (13) and observing that we can further factor $p(\boldsymbol{\theta})$ in (23) as

$$p(\boldsymbol{\theta}) = p(\theta_0)\prod_{n=1}^{N-1} p(\theta_n|\theta_{n-1}) \quad (26)$$

where $p(\theta_n|\theta_{n-1})$ is a Gaussian pdf in θ_n with mean θ_{n-1} and variance σ_Δ^2, we obtain

$$p(\boldsymbol{\alpha}, \boldsymbol{\phi}, \boldsymbol{\theta}|\mathbf{r}) \,\widetilde{\propto}\, P(\phi_{-1})p(\theta_0)\prod_{n=0}^{N-1} I_n(\phi_n, \phi_{n-1}, \alpha_n) \cdot P(\alpha_n)H_n(\alpha_n, \phi_{n-1}, \theta_n)\prod_{n=1}^{N-1} p(\theta_n|\theta_{n-1}) \quad (27)$$

which is exact except for the approximation (21) and that related to the use of the principal components only. In the following, we will denote a Gaussian pdf in the variable x, with mean η and variance ρ^2, as $g(\eta, \rho^2; x)$. Hence, $p(\theta_n|\theta_{n-1}) = g(\theta_{n-1}, \sigma_\Delta^2; \theta_n)$.

The FG corresponding to (27) has cycles. However, by clustering [19] the variables θ_n and ϕ_{n-1}, i.e., defining $\sigma_n = (\phi_{n-1}, \theta_n)$, we obtain the FG in Fig. 2. Since this new FG does not contain cycles, by applying to it the SPA with a *non-iterative* forward-backward schedule, we obtain, except for the above mentioned approximations, the exact a posteriori probabilities $P(\alpha_n|\mathbf{r})$ necessary to implement the MAP *symbol* detection strategy. With reference to the messages in the figure, the resulting forward–backward algorithm is characterized by

the following recursions and completion:

$$\nu_{f,n+1}(\phi_n,\theta_{n+1}) = \sum_{\alpha_n} P(\alpha_n) \int \nu_{f,n}(\check{\phi}_{n-1},\theta_n) \cdot H_n(\alpha_n,\check{\phi}_{n-1},\theta_n) g(\theta_n,\sigma_\Delta^2;\theta_{n+1}) d\theta_n \tag{28}$$

$$\nu_{b,n}(\phi_{n-1},\theta_n) = \sum_{\alpha_n} P(\alpha_n) H_n(\alpha_n,\phi_{n-1},\theta_n) \cdot \int \nu_{b,n+1}(\check{\check{\phi}}_n,\theta_{n+1}) g(\theta_n,\sigma_\Delta^2;\theta_{n+1}) d\theta_{n+1} \tag{29}$$

$$P_e(\alpha_n) = \sum_{\phi_n} \iint \nu_{f,n}(\check{\phi}_{n-1},\theta_n)\nu_{b,n+1}(\phi_n,\theta_{n+1}) \cdot H_n(\alpha_n,\check{\phi}_{n-1},\theta_n) g(\theta_n,\sigma_\Delta^2;\theta_{n+1}) d\theta_n d\theta_{n+1} \tag{30}$$

with the following initial conditions: $\nu_{f,0}(\phi_{-1},\theta_0) = 1/(p2\pi)$ and $\nu_{b,N}(\phi_{N-1},\theta_N) = 1/(p2\pi)$.

A proof of the following properties is given in the Appendix:

Property 1: for each $\ell = 0,\ldots,p-1$,

$$\nu_{f,n}([\phi_{n-1}+\ell]_p,\theta_n) = \nu_{f,n}(\phi_{n-1},\theta_n + 2\pi h\ell) \tag{31}$$

$$\nu_{b,n}([\phi_{n-1}+\ell]_p,\theta_n) = \nu_{b,n}(\phi_{n-1},\theta_n + 2\pi h\ell)\,. \tag{32}$$

Property 2: The extrinsic information in (30) is given by the sum of p terms (one for each value of ϕ_n). All these terms assume the same value, i.e., they do not depend on ϕ_n, for each given α_n.

From the first property it follows that it is not necessary to evaluate and store all pdfs $\nu_{f,n}(\phi_{n-1},\theta_n)$ and $\nu_{b,n}(\phi_{n-1},\theta_n)$ for different values of ϕ_{n-1}. It is for instance sufficient to evaluate $\bar{\nu}_{f,n}(\theta_n) = \nu_{f,n}(\phi_{n-1}=0,\theta_n)$ and $\bar{\nu}_{b,n}(\theta_n) = \nu_{b,n}(\phi_{n-1}=0,\theta_n)$. From the second property, it follows that only one term in (30) needs to be evaluated. The MAP symbol detection strategy can therefore be simplified as follows:

$$\bar{\nu}_{f,n+1}(\theta_{n+1}) = \sum_{\alpha_n} P(\alpha_n) \int \bar{\nu}_{f,n}(\theta_n - 2\pi h\bar{\alpha}_n) \cdot H_n(\alpha_n,\phi_{n-1}=[-\bar{\alpha}_n]_p,\theta_n) g(\theta_n,\sigma_\Delta^2;\theta_{n+1}) d\theta_n \tag{33}$$

$$\bar{\nu}_{b,n}(\theta_n) = \sum_{\alpha_n} P(\alpha_n) H_n(\alpha_n,\phi_{n-1}=0,\theta_n) \cdot \int \bar{\nu}_{b,n+1}(\theta_{n+1}+2\pi h\bar{\alpha}_n) g(\theta_n,\sigma_\Delta^2;\theta_{n+1}) d\theta_{n+1} \tag{34}$$

$$P_e(\alpha_n) \propto \iint \bar{\nu}_{f,n}(\theta_n)\bar{\nu}_{b,n+1}(\theta_{n+1}+2\pi h\bar{\alpha}_n) \cdot H_n(\alpha_n,\phi_{n-1}=0,\theta_n) g(\theta_n,\sigma_\Delta^2;\theta_{n+1}) d\theta_n d\theta_{n+1} \tag{35}$$

with the following initial conditions: $\bar{\nu}_{f,0}(\theta_0) = 1/2\pi$ and $\bar{\nu}_{b,N}(\theta_N) = 1/2\pi$. Hence, we have a single forward-backward estimator of the phase probability density function and a final completion.

This exact MAP symbol detection strategy involves integration and computation of continuous pdfs, and it is not suited for direct implementation. A solution for this problem is suggested in [26] and consists of the use of *canonical distributions*, i.e., the pdfs $\bar{\nu}_{f,n}(\theta_n)$ and $\bar{\nu}_{b,n}(\theta_n)$ computed by the algorithm are constrained to be in a certain "canonical" family, characterized by some parameterization. Hence, the forward and backward recursions reduce to propagating and updating the parameters of the pdf rather than the pdf itself. Two algorithms based on this approach will be now described.

A. Proposed Algorithms

1) First Algorithm: A very straightforward solution to implement (33) and (34) is obtained by discretizing the channel phase [20], [22]. In this way, the pdfs $\bar{\nu}_{f,n}(\theta_n)$ and $\bar{\nu}_{b,n}(\theta_n)$ become probability mass functions (pmfs) and the integrals in (33), (34), and (35) become summations. When the number D of discretization levels is large enough, the resulting algorithm becomes optimal (in the sense that its performance approaches that of the exact algorithm).[7] Hence, it may be used to obtain a performance benchmark and will be denoted to as "discretized-phase algorithm" (*dp-algorithm*).

2) Second Algorithm: By observing that the Tikhonov distribution ensures a very good performance with a low complexity when used as a canonical distribution in detection algorithms for phase noise channels [22], pdfs $\bar{\nu}_{f,n}(\theta_n)$ and $\bar{\nu}_{b,n}(\theta_n)$ are constrained to have the following expressions

$$\bar{\nu}_{f,n}(\theta_n) = \sum_{m=0}^{p-1} q_{f,n}^{(m)} t\left(z_{f,n};\theta_n - 2\pi hm\right) \tag{36}$$

$$\bar{\nu}_{b,n}(\theta_n) = \sum_{m=0}^{p-1} q_{b,n}^{(m)} t\left(z_{b,n};\theta_n - 2\pi hm\right) \tag{37}$$

where, for each time index n, $\{q_{f,n}^{(m)}, m=0,1,\ldots,p-1\}$ ($\{q_{b,n}^{(m)}, m=0,1,\ldots,p-1\}$) and $z_{f,n}$ ($z_{b,n}$) are, respectively, p real coefficients and one complex coefficient, and $t(z;\theta)$ is a Tikhonov distribution with complex parameter z defined as

$$t(z;\theta) = \frac{e^{\mathrm{Re}\left[ze^{-j\theta}\right]}}{2\pi \mathrm{I}_0(|z|)} \tag{38}$$

$\mathrm{I}_0(x)$ being the zero-th order modified Bessel function of the first kind. Note that $\sum_{m=0}^{p-1} q_{f/b,n}^{(m)} = 1$ in order to obtain pdfs.

Three approximations are now introduced in order to derive the proposed detection algorithm:[8]

i. the convolution of a Tikhonov and a Gaussian pdf is still a Tikhonov pdf, with a modified complex parameter [22], i.e.,

$$\int t(z;x)g(x,\rho^2;y)dx \simeq t\left(\frac{z}{1+\rho^2|z|};y\right) \tag{39}$$

ii. since, for large arguments, $\mathrm{I}_0(x) \simeq e^x$, we approximate

$$e^{\mathrm{Re}[ze^{-j\theta}]} \simeq 2\pi e^{|z|} t(z;\theta) \tag{40}$$

iii. let z be a complex number, $\{u_m, m=0,1,\ldots,p-1\}$ a set of complex numbers, and $\{q_m, m=0,1,\ldots,p-1\}$ a set of real numbers such that $\sum_m q_m = 1$, then the following approximation holds, especially when $|z|$ is sufficiently larger than each $|u_m|$ or when there is a $\overline{m}$ such that $q_{\overline{m}} \gg q_m$, $\forall m \neq \overline{m}$:

$$\sum_m q_m t\left(ze^{j2\pi hm} + u_m;\theta\right) \simeq \sum_m q_m t\left(we^{j2\pi hm};\theta\right) \tag{41}$$

where $w = z + \sum_\ell q_\ell u_\ell e^{-j2\pi h\ell}$.

In order to illustrate the derivation of the proposed algorithm, we consider the case of a binary modulation, i.e.,

[7] As a rule of thumb (confirmed by the results in [20]), the number of discretization levels must be at least $D = 8p$ in order to avoid any performance loss.

[8] A justification of these approximations is represented by the excellent performance of the resulting algorithm.

$M = 2$, and hence $K = 1$, although the generalization to the non-binary case is straightforward from a conceptual viewpoint.[9] In this case

$$\frac{1}{N_0}\sum_{k=0}^{K-1} x_{k,n}a_{k,n}^* = \frac{1}{N_0}x_{0,n}a_{0,n}^* = y_n e^{-j2\pi h\phi_n} \tag{42}$$

where we define $y_n = \frac{1}{N_0}x_{0,n}e^{j\pi h(n+1)(M-1)}$. We now derive the reduced-complexity forward recursion. Substituting (25) in (33) and assuming that $\bar{\nu}_{f,n-1}(\theta_{n-1})$ has the canonical expression (36), we obtain

$$\bar{\nu}_{f,n+1}(\theta_{n+1}) = \sum_{\alpha_n} P(\alpha_n) \sum_{m=0}^{p-1} q_{f,n}^{(m)} \int g(\theta_n, \sigma_\Delta^2; \theta_{n+1}) \cdot t\left(z_{f,n}; \theta_n - 2\pi h(\bar{\alpha}_n + m)\right) e^{\mathrm{Re}\left[y_n e^{-j\theta_n}\right]} d\theta_n \,. \tag{43}$$

By now changing the first summation index in $\ell = m + \bar{\alpha}_n$, using (39) and (40), discarding irrelevant multiplicative factors, and neglecting $|y_n|$ with respect to $|z_{f,n}|$, we have

$$\bar{\nu}_{f,n+1}(\theta_{n+1}) = \sum_{\ell}\left[\sum_{\alpha_n} P(\alpha_n) q_{f,n}^{([\ell-\bar{\alpha}_n]_p)}\right] \cdot e^{\left|z_{f,n}+y_n e^{-j2\pi h\ell}\right|} t\left(\frac{z_{f,n}e^{j2\pi h\ell}+y_n}{1+\sigma_\Delta^2|z_{f,n}|}; \theta_n\right) \tag{44}$$

This resulting $\bar{\nu}_{f,n+1}(\theta_{n+1})$ is not in the constrained form (36). However, by applying the approximation (41), we obtain the following updating equations for the parameters of the canonical distribution (36)

$$q_{f,n+1}^{(\ell)} \propto \left[\sum_{\alpha_n} P(\alpha_n) q_{f,n}^{([\ell-\bar{\alpha}_n]_p)}\right] e^{\left|z_{f,n}+y_n e^{-j2\pi h\ell}\right|} \tag{45}$$

$$z_{f,n+1} = \frac{z_{f,n} + y_n \sum_m q_{f,n+1}^{(m)} e^{-j2\pi hm}}{1+\sigma_\Delta^2|z_{f,n}|} \,. \tag{46}$$

It is worth noticing that, before the evaluation of the coefficient $z_{f,n+1}$, the p real coefficients $q_{f,n+1}^{(\ell)}$, evaluated through (45), have to be normalized so that their sum is 1. Since there is no a priori knowledge of the initial phase or of the initial symbol $a_{0,-1}$, the following initial values of the recursive coefficients result

$$\begin{aligned} q_{f,0}^{(\ell)} &= 1/p \\ z_{f,0} &= 0 \,. \end{aligned}$$

In addition, since at the first step of the forward recursion the approximation (41) does not hold, we use the following values for the recursive coefficients at time $n = 1$:

$$\begin{aligned} q_{f,1}^{(\ell)} &= \delta_\ell \\ z_{f,1} &= \frac{y_0}{1+\sigma_\Delta^2|y_0|} \end{aligned}$$

where δ_ℓ represents the Kronecker delta.

[9]Some non-binary examples will be considered in the numerical results.

Similarly, it is also possible to find the backward recursive equations. We report the final expressions only:

$$u(\alpha_n; m) = \frac{P(\alpha_n) q_{b,n+1}^{([m]_p)} e^{\left|z'_{b,n+1}+y_n e^{-j2\pi hm}\right|}}{\sum_\ell \sum_\alpha P(\alpha) q_{b,n+1}^{(\ell)} e^{\left|z'_{b,n+1}+y_n e^{-j2\pi h\ell}\right|}}$$

$$q_{b,n}^{(\ell)} = \sum_{\alpha_n} u(\alpha_n; \ell + \bar{\alpha}_n) \tag{47}$$

$$z_{b,n} = z'_{b,n+1} + y_n \sum_m \left(\sum_{\alpha_n} u(\alpha_n; m)\right) e^{-j2\pi hm} \tag{48}$$

where $z'_{b,n+1} = \frac{z_{b,n+1}}{1+\sigma_\Delta^2|z_{b,n+1}|}$ and coefficients $u(\cdot;\cdot)$ have been introduced to simplify the notation (they do not need to be stored, since they are not involved in the completion stage). The initial values of the backward coefficients are

$$q_{b,N}^{(\ell)} = 1/p \qquad q_{b,N-1}^{(\ell)} = \begin{cases} P(\alpha_{N-1} = -1) & \ell = 0 \\ P(\alpha_{N-1} = +1) & \ell = p-1 \\ 0 & \text{else} \end{cases}$$

$$z_{b,N} = 0 \qquad z_{b,N-1} = y_{N-1}$$

Finally, substituting (36) and (37) into (35) and discarding irrelevant constants, the extrinsic information is evaluated as

$$P_e(\alpha_n) \propto \sum_\ell \sum_m q_{f,n}^{(\ell)} q_{b,n+1}^{(m)} \cdot \exp\left(\left|z_{f,n}e^{j2\pi h(\ell+\bar{\alpha}_n)} + z'_{b,n+1}e^{j2\pi hm} + y_n\right|\right) \,. \tag{49}$$

In summary, this detection algorithm is based on three steps: a forward recursion in which, for each time epoch n, one complex and p real coefficients are evaluated based on (45) and (46), a backward recursion, based on (47) and (48), which proceeds similarly, and finally a completion (49), which consists of the sum of p^2 terms (although only a small amount of them can be numerically significant). This algorithm will be denoted to as "algorithm based on Tikhonov parameterization" (*Tikh-algorithm*).

B. Complexity Considerations

We address the computational complexity of the proposed algorithms. We assume that the computation of a non linear function is performed by using a look-up table (LUT). Table I presents the computational complexity in terms of number of operations (additions and multiplications) between two real arguments, accesses to LUT, and memory requirements to store the computed coefficients, per CPM symbol. The computational complexity of the front-end processing is not considered, being the same for both algorithms. From the table, it is clear that the *Tikh-algorithm* has a much lower complexity with respect to the *dp-algorithm* and, in fact, this latter algorithm must be considered only as a performance benchmark.

V. Numerical Results

In this section, the performance of the proposed detection schemes is assessed by computer simulations in terms of bit error rate (BER) versus E_b/N_0, E_b being the received signal

TABLE I
COMPUTATIONAL LOAD PER CPM SYMBOL OF THE PROPOSED ALGORITHMS.

	Tikhonov	dp-BCJR
Operations	$p(13pM + 6M + 12)$	$52MD$
LUT accesses	$p(3pM + 2)$	$9MD$
Memory requirement	$p + 2$	pD

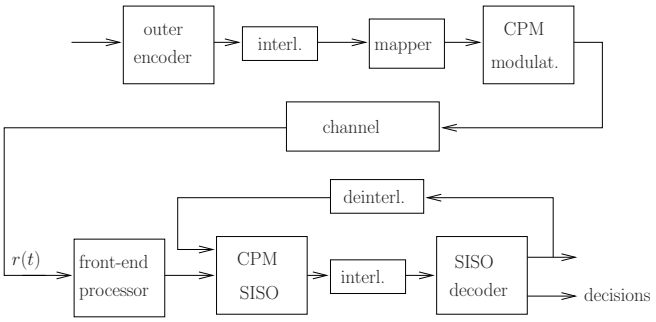

Fig. 3. Transmitter and receiver structure for the considered SCCPM schemes.

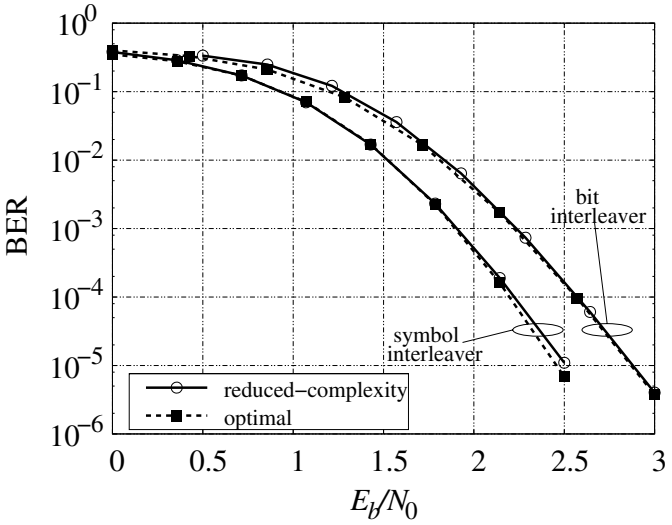

Fig. 4. Concatenated 2RC modulation with $h = 1/4$ and $M = 4$.

energy per information bit. To evaluate the quality of the soft-outputs produced by the MAP *symbol* detection algorithms with reduced complexity, we consider serially concatenated CPM (SCCPM) schemes with iterative decoding. The relevant system model is depicted in Fig. 3. The considered concatenated schemes are completely defined by the outer code description, the codeword length, the type of interleaver (bit or symbol), the type of mapping, the CPM parameters, and finally the total number of iterations for the iterative decoding process. No pilot symbols or a known preamble have been inserted.

In our computer simulations, five different SCCPM schemes, whose details are summarized in Table II, are considered. The outer codes of the first four schemes have been chosen following the guidelines in [29], while the nonsystematic irregular repeat-accumulate code of the fifth scheme has been designed by means of the extrinsic information transfer (EXIT) charts following the method in [30] (see also [31]). Note that, in this latter case, the outer code is indeed a low-density generator matrix (LDGM) composed by the serial concatenation of a repetition stage, an interleaver and a parity generator. It is not necessary to explicitly insert the accumulator after the LDGM, since it is embedded in the CPM modulation.

In Fig. 4 we consider the concatenation of a non-recursive rate-1/2 convolutional code (CC) with generators $G_1 = 7$ and $G_2 = 5$ (octal notation) and a quaternary raised-cosine (RC) modulation [1] with frequency pulse of duration $L = 2$ symbol intervals (2RC) and modulation index $h = 1/4$. The phase is considered known to the receiver. Two coded bits are mapped into one CPM symbol by using Gray mapping. In the case of the considered 2RC modulation, we have $M - 1 = 3$ principal components but, observing that two principal pulses are almost identical, a front-end composed of only two filters is sufficient. The reduced-complexity soft-output detector, based on the algorithm described in Section III, has only $p = 4$ states whereas the optimal detector has $pM^{L-1} = 16$ states. A symbol interleaver of length 1024 symbols and a bit interleaver of length 2048 bits are considered and 20 iterations are performed.[10] In [5] some considerations have been carried out about the advantages and disadvantages, in terms of convergence threshold and error floor, of symbol interleavers with respect to bit interleavers in SCCPM schemes. In particular, it has been shown that systems with symbol interleaving usually have a lower convergence threshold and a higher error floor. In our simulation, due to the use of the DRP interleaver, the error floor does not appear, but the result on the convergence threshold is confirmed. In any case, it can be observed that, independently of the used interleaver, the proposed reduced-complexity coherent receiver exhibits a negligible performance loss with respect to the optimal MAP symbol detection algorithm.

Similar considerations hold for Fig. 5 which refers to a different SCCPM scheme, i.e., the concatenation of a non-recursive rate-2/3 convolutional code (CC) with generators $G_1 = 32$, $G_2 = 21$, and $G_3 = 31$, and a 2RC modulation with $h = 1/6$ and $M = 8$. Hence, in this case the spectral efficiency is of 2 bits per channel use. For this modulation format, we have $M - 1 = 7$ principal components but a front-end composed of only 3 filters is sufficient. The number of states of the proposed detector is $p = 6$, whereas the optimal receiver has $pM^{L-1} = 48$ states. A length-2048 symbol interleaver and a length-6144 bit interleaver are considered and 20 iterations are performed.

In Fig. 6 and Fig. 7 the effect of a time-varying phase, unknown to the receiver and modeled as a Wiener process with standard deviation σ_Δ equal to 5 and 15 degrees, is considered. Fig. 6 refers to the serial concatenation of a 4-state rate-1/2 CC, with generators $G_1 = 7$ and $G_2 = 5$, and the minimum shift keying (MSK) modulation, i.e., a binary modulation with $h = 1/2$ and a rectangular frequency pulse of duration T (1REC). Hence, in this case a single linearly modulated component perfectly describes the CPM signal and

[10] A dithered relative prime (DRP) interleaver [32] is used in both cases.

TABLE II
DETAILS OF THE CONSIDERED SCCPM SCHEMES.

Fig.	Pulse	M	h	Mapping	Outer code	Codeword length	Interleaver	Iterations
4	2RC	4	$1/4$	Gray	CC (7,5) $R=1/2$	2048	Bit or Symbol	20
5	2RC	8	$1/6$	Gray	CC (32,21,31) $R=2/3$	6144	Bit or Symbol	20
6	1REC	2	$1/2$	-	CC (7,5) $R=1/2$	2048	Bit	10
7	2RC	4	$2/3$	Natural	CC (7,5) $R=1/2$	2048	Bit	15
8	2RC	2	$1/4$	-	Repeat-Accumulate $R=2/3$	8100	Bit[a]	50

[a]In this case, the bit interleaver is embedded in the Repeat-Accumulate encoder.

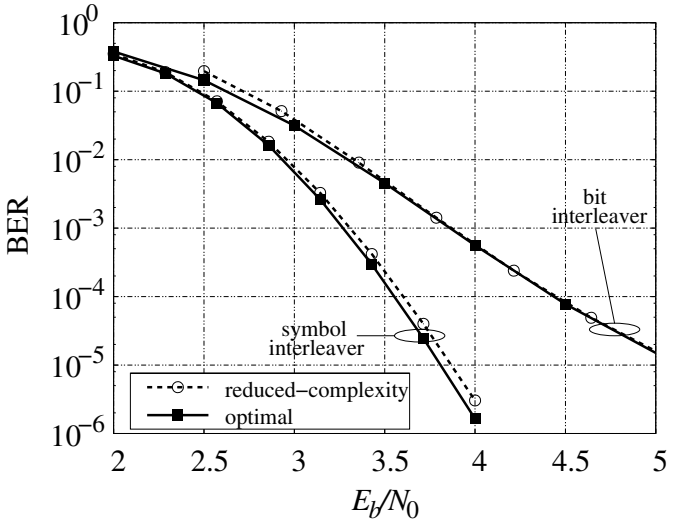

Fig. 5. Concatenated 2RC modulation with $h = 1/6$ and $M = 8$.

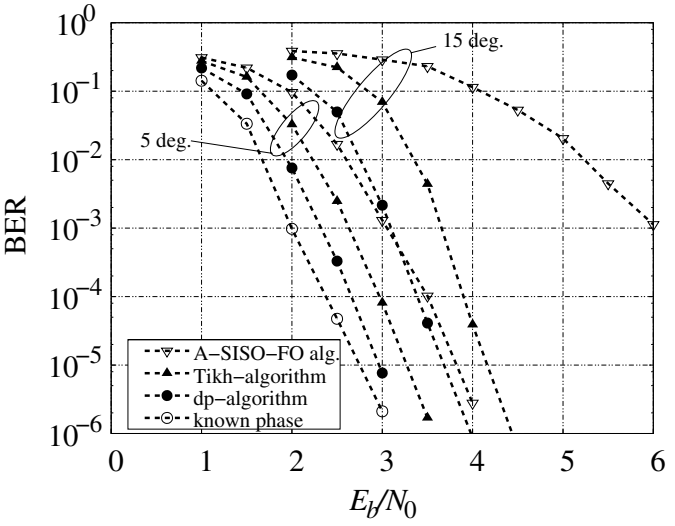

Fig. 6. Concatenated MSK modulation.

hence the optimal and reduced-complexity receivers coincide. An interleaver of length 2048 bits is used and a maximum of 10 iterations is allowed. The performance of the proposed *dp-algorithm* and *Tikh-algorithm* is shown and compared with that of the adaptive soft-input soft-output forward-only (A-SISO-FO) algorithm described in [24]. $D = 16$ discretization levels have been used for the *dp-algorithm* and no performance improvement has been observed for larger values of D. The ideal curve related to the perfect knowledge of the channel phase is also shown for comparison. It can be observed that, at a BER of 10^{-5} and for $\sigma_\Delta = 5$ degrees, the loss of the optimal *dp-algorithm* with respect to the known-phase case is approximately 0.25 dB, while the loss of the low-complexity *Tikh-algorithm* is about 0.5 dB. More than 0.5 dB is gained by the *Tikh-algorithm* with respect to the algorithm in [24]. For $\sigma_\Delta = 15$ degrees, the performance loss of all the algorithms is obviously larger but, even in this case, the advantage of the *Tikh-algorithm* with respect to the A-SISO-FO algorithm is evident.

Among the algorithms described in [24], we consider here only the A-SISO-FO algorithm for which the phase is estimated during the forward recursion only. The reason is that it exhibits a better performance with respect to the algorithms based on independent forward and backward estimates since the latter are difficult to combine due to phase slips [24]. This is not surprising since the A-SISO algorithms proposed in [24] are derived based on a "reasonable approximation" commonly used when the unknown parameters are modeled as deterministic (see [24, eqn. (4)]). Hence, in this case an "optimal" algorithm, in the sense of the symbol error rate minimization, is not defined, and only heuristic approaches (such as those proposed in [24]) can be adopted. On the contrary, we consider a Bayesian model of the phase noise. Hence, in this case the optimal detection strategy is defined and, as demonstrated, this strategy is based on forward and backward Bayesian estimators which are properly combined. The proposed algorithms derive from it through (minor) approximations and for them there is no benefit in using a forward-only estimator.

Fig. 7 refers to the concatenation of the same CC used in the previous figure with a quaternary 2RC modulation with $h = 2/3$. Hence, $M - 1 = 3$ principal pulses need to be considered and the number of states of the reduced-complexity receivers is $p = 3$. A bit interleaver of length 2048 bits is used, the natural mapping is adopted to map a couple of bits into a CPM symbol, and, at the receiver, a maximum of 15 iterations is allowed. For a Wiener phase noise with $\sigma_\Delta = 5$ degrees, the performance of the *dp-algorithm* (with $D = 24$) and that of the *Tikh-algorithm* is shown and compared with that of the A-SISO-FO algorithm and that of the ideal case of perfectly known phase, for both the reduced-complexity and optimal MAP symbol detection. Even in this case, the loss exhibited by the proposed detection schemes is limited and they outperform the A-SISO-FO algorithm.

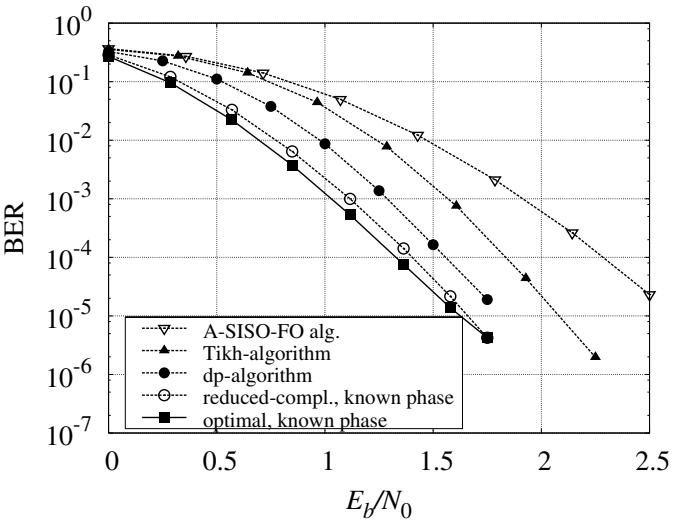

Fig. 7. Concatenated 2RC modulation with $h = 2/3$ and $M = 4$.

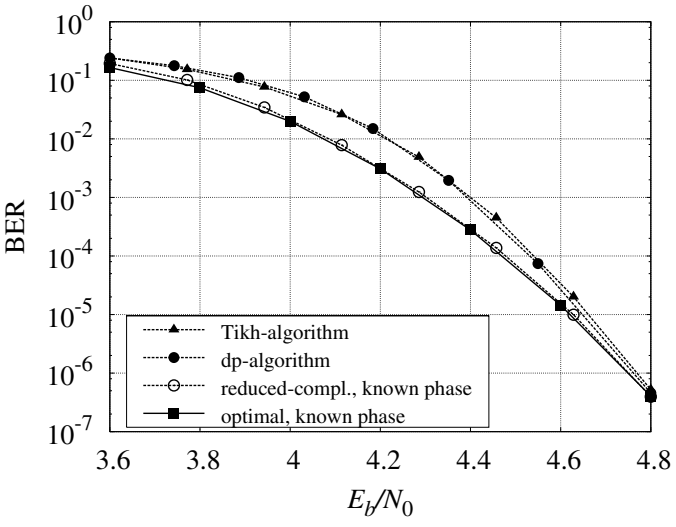

Fig. 8. Concatenated 2RC modulation with $h = 1/4$ and $M = 2$.

For a complete picture, with reference to the CPM schemes in Fig. 6 and Fig. 7 we compare the computational complexity of the proposed schemes with that of A-SISO-FO algorithm. The computational load is computed per CPM symbol per iteration and the contribution of the front-end processing is not considered (although for the proposed algorithms it is lower). From Table III it can be observed that the *Tikh-algorithm* has a complexity comparable to that of the A-SISO-FO algorithm for the case of the MSK modulation, but it is simpler for the quaternary 2RC modulation case and its complexity advantage increases for higher values of M and/or L.

Finally, in Fig. 8 we consider, as outer code, a properly designed irregular nonsystematic repeat-accumulate of rate $R = 2/3$ and codewords of 8100 bits, concatenated with a binary 2RC CPM with $h = 1/4$. The optimized degree distributions of the considered RA code are reported in Table IV. Its convergence threshold, obtained by means of EXIT charts analysis, is $3.47\,\mathrm{dB}$. A different phase noise model is adopted in this case, namely a model recently proposed for consumer grade equipments to be employed in the next generation digital video broadcasting satellite systems (DVB-S2), assuming a baud rate of 10 Mbaud [22]. Although the Wiener model does not apply to this case, for the proposed detectors a properly optimized value of $\sigma_\Delta = 0.5$ degrees has been used. For comparison purposes we also added the simulation results for the ideal case of perfectly known phase. In all cases a maximum of 50 iterations is performed. Despite the model mismatch, both the proposed *dp-algorithm* (with $D = 32$ discretization levels) and *Tikh-algorithm* exhibit a loss of less than 0.05 dB at a BER of 10^{-5} even if, for increasing L and decreasing h, the resulting CPM modulation has a much higher sensitivity to phase noise.

TABLE IV
DEGREE DISTRIBUTIONS OF THE CONSIDERED RA CODE.

Repetition		Parity	
degree	rate	degree	rate
3	0.8477	1	0.8000
13	0.1056	4	0.2000
25	0.0467		

VI. CONCLUSIONS

In this paper, the problem of MAP *symbol* detection for CPM signals transmitted over coherent and phase noise channels has been faced. The proposed algorithms have been derived based on factor graphs and the sum-product algorithm and using the Laurent representation of a CPM signal as sum of linearly modulated components. In particular, only the principal components have been considered, since neglecting the other components only a minor degradation results. The derived low-complexity algorithms are fundamental to implement iterative decoding receivers for high-order partial response CPM formats.

For the phase noise channel, it has been shown that simplified MAP *symbol* detection can be implemented based on a forward-backward single estimation of the phase probability density function and a final completion. For the practical implementation of the forward-backward estimator, two algorithms have been proposed. The first one is based on the phase discretization and becomes optimal for a large enough number of discretization levels. To reduce the computational complexity, some approximations have been introduced in order to derive a new algorithm which exhibits a very good performance and a much lower complexity.

APPENDIX I
PROOF OF THE PROPERTIES

In this appendix, we prove the properties introduced in Section IV. For the first property, we concentrate on the forward recursion, since the extension to the backward recursion is trivial. This property can be demonstrated by induction. First of all, property (31) holds for $n = 0$, since $\nu_{f,0}(\phi_{-1}, \theta_0) = P(\phi_{-1})p(\theta_0) = 1/(p2\pi)$. Hence, it satisfies the property. We now suppose that the property is true for a given n and we prove that it is true also for $n + 1$. By evaluating (28) for $\check{\phi}_n = [\phi_n + \ell]_p$, observing that if $(\phi_n, \check{\phi}_{n-1}, \alpha_n)$ satisfy (7), then $([\phi_n + \ell]_p, [\check{\phi}_{n-1} + \ell]_p, \alpha_n)$ satisfy as well (see (7)),

TABLE III

COMPUTATIONAL LOAD PER CPM SYMBOL PER ITERATION, FOR THE CPM SIGNALS CONSIDERED IN FIG. 6 AND FIG. 7.

	Fig. 6			Fig. 7		
	Tikhonov	dp-BCJR	A-SISO-FO	Tikhonov	dp-BCJR	A-SISO-FO
Operations	152	1664	112	576	4992	1344
LUT accesses	28	288	48	114	864	576
Memory requirement	4	32	4	5	72	24

and that $H_n(\alpha_n, \phi_{n-1} + \ell, \theta_n) = H_n(\alpha_n, \phi_{n-1}, \theta_n + 2\pi h\ell)$ (see (7), (25), and the expression of $a_{k,n}$ as a function of $a_{0,n-1}$ and α_n in [12]), and finally using the Property 1 for $\nu_{f,n}(\phi_{n-1}, \theta_n)$, we obtain

$$\nu_{f,n+1}(\dot{\phi}_n, \theta_{n+1}) = \sum_{\alpha_n} P(\alpha_n) \int \nu_{f,n}(\check{\phi}_{n-1}, \theta_n + 2\pi h\ell) \cdot H_n(\alpha_n, \check{\phi}_{n-1}, \theta_n + 2\pi h\ell) g(\theta_n, \sigma_\Delta^2; \theta_{n+1}) d\theta_n \,. \quad \text{(A1)}$$

Now, by applying to the integral the change of variable $\psi_n = \theta_n + 2\pi h\ell$ and noting that, for each angle ϵ, $g(\theta_n - \epsilon, \sigma_\Delta^2; \theta_{n+1}) = g(\theta_n, \sigma_\Delta^2; \theta_{n+1} + \epsilon)$, the Property 1 for $\nu_{f,n+1}(\phi_n, \theta_{n+1})$ easily follows.

We now take into account the second property. The completion (30) is of the form

$$P_e(\alpha_n) = \sum_{\phi_n} \Phi(\phi_n; \alpha_n) \quad \text{(A2)}$$

where the expressions of the terms $\Phi(\phi_n; \alpha_n)$ can be easily obtained by comparing (A2) with (30). We now prove that, for any given α_n, $\Phi(\phi_n; \alpha_n)$ does not depend on ϕ_n. By computing $\Phi(\phi_n; \alpha_n)$ for $\dot{\phi}_n = [\phi_n + \ell]_p$ and using (31) and (32), we have

$$\Phi(\dot{\phi}_n; \alpha_n) = \iint \nu_{f,n}(\check{\phi}_{n-1}, \theta_n + 2\pi h\ell) \cdot \nu_{b,n+1}(\phi_n, \theta_{n+1} + 2\pi h\ell) H_n(\alpha_n, \check{\phi}_{n-1}, \theta_n + 2\pi h\ell) \cdot g(\theta_n, \sigma_\Delta^2; \theta_{n+1}) d\theta_n d\theta_{n+1} \quad \text{(A3)}$$

from which, after a change of variable in the integrals, it follows that

$$\Phi(\dot{\phi}_n; \alpha_n) = \Phi(\phi_n; \alpha_n) \,. \quad \text{(A4)}$$

REFERENCES

[1] J. Anderson, T. Aulin, and C.-E. Sundberg, *Digital Phase Modulation*. New York: Plenum Press, 1986.

[2] K. R. Narayanan and G. L. Stüber, "Performance of trellis-coded CPM with iterative demodulation and decoding," *IEEE Trans. Commun.*, vol. 49, pp. 676–687, Apr. 2001.

[3] P. Moqvist and T. M. Aulin, "Serially concatenated continuous phase modulation with iterative decoding," *IEEE Trans. Commun.*, vol. 49, pp. 1901–1915, Nov. 2001.

[4] B. E. Rimoldi, "A decomposition approach to CPM," *IEEE Trans. Inf. Theory*, vol. 34, pp. 260–270, Mar. 1988.

[5] M. Xiao and T. M. Aulin, "Serially concatenated continuous phase modulation with symbol interleavers: performance, properties and design principles," in *Proc. IEEE Global Telecommun. Conf.*, pp. 179–183, Nov.-Dec. 2004.

[6] G. Colavolpe, G. Ferrari, and R. Raheli, "Reduced-state BCJR-type algorithms," *IEEE J. Sel. Areas Commun.*, vol. 19, pp. 848–859, May 2001.

[7] R. Balasubramanian, M. P. Fitz, and J. K. Krogmeier, "Optimal and suboptimal symbol-by-symbol demodulation of continuous phase modulated signals," *IEEE Trans. Commun.*, vol. 46, pp. 1662–1668, Dec. 1998.

[8] J. Huber and W. Liu, "An alternative approach to reduced-complexity CPM-receivers," *IEEE J. Sel. Areas Commun.*, vol. 7, pp. 1437–1449, Dec. 1989.

[9] W. Tang and E. Shwedyk, "ML estimation of symbol timing and carrier phase for CPM in Walsh signal space," *IEEE Trans. Commun.*, vol. 49, pp. 969–974, June 2001.

[10] P. Moqvist and T. Aulin, "Orthogonalization by principal components applied to CPM," *IEEE Trans. Commun.*, vol. 51, pp. 1838–1845, Nov. 2003.

[11] P. A. Laurent, "Exact and approximate construction of digital phase modulations by superposition of amplitude modulated pulses (AMP)," *IEEE Trans. Commun.*, vol. 34, pp. 150–160, Feb. 1986.

[12] U. Mengali and M. Morelli, "Decomposition of M-ary CPM signals into PAM waveforms," *IEEE Trans. Inf. Theory*, vol. 41, pp. 1265–1275, Sept. 1995.

[13] G. Colavolpe and R. Raheli, "Reduced-complexity detection and phase synchronization of CPM signals," *IEEE Trans. Commun.*, vol. 45, pp. 1070–1079, Sept. 1997.

[14] G. Ungerboeck, "Adaptive maximum likelihood receiver for carrier-modulated data-transmission systems," *IEEE Trans. Commun.*, vol. com-22, pp. 624–636, May 1974.

[15] G. Colavolpe and R. Raheli, "Noncoherent sequence detection of continuous phase modulations," *IEEE Trans. Commun.*, vol. 47, pp. 1303–1307, Sept. 1999.

[16] G. D. Forney, Jr., "Lower bounds on error probability in the presence of large intersymbol interference," *IEEE Trans. Commun.*, vol. 20, pp. 76–77, Feb. 1972.

[17] L. R. Bahl, J. Cocke, F. Jelinek, and J. Raviv, "Optimal decoding of linear codes for minimizing symbol error rate," *IEEE Trans. Inf. Theory*, vol. 20, pp. 284–287, Mar. 1974.

[18] G. Colavolpe and A. Barbieri, "On MAP symbol detection for ISI channels using the Ungerboeck observation model," *IEEE Commun. Lett.*, vol. 9, pp. 720–722, Aug. 2005.

[19] F. R. Kschischang, B. J. Frey, and H.-A. Loeliger, "Factor graphs and the sum-product algorithm," *IEEE Trans. Inf. Theory*, vol. 47, pp. 498–519, Feb. 2001.

[20] M. Peleg, S. Shamai (Shitz), and S. Galán, "Iterative decoding for coded noncoherent MPSK communications over phase-noisy AWGN channel," *IEE Proc. Commun.*, vol. 147, pp. 87–95, Apr. 2000.

[21] A. Anastasopoulos and K. M. Chugg, "Adaptive iterative detection for phase tracking in turbo coded systems," *IEEE Trans. Commun.*, vol. 49, pp. 2135–2144, Dec. 2001.

[22] G. Colavolpe, A. Barbieri, and G. Caire, "Algorithms for iterative decoding in the presence of strong phase noise," *IEEE J. Sel. Areas Commun.*, vol. 23, pp. 1748–1757, Sept. 2005.

[23] Q. Zhao, H. Kim, and G. L. Stüber, "Adaptive iterative phase synchronization for serially concatenated continuous phase modulation," in *Proc. IEEE Military Comm. Conf. (MILCOM)*, pp. 78–83, Oct. 2003.

[24] Q. Zhao, H. Kim, and G. L. Stüber, "Innovation-based MAP estimation with application to phase synchronization for serially concatenated CPM," *IEEE Trans. Wireless Commun.*, vol. 5, pp. 1033–1043, May 2006.

[25] A. Anastasopoulos and K. M. Chugg, "Adaptive soft-input soft-output algorithms for iterative detection with parametric uncertainty," *IEEE Trans. Commun.*, vol. 48, pp. 1638–1649, Oct. 2000.

[26] A. P. Worthen and W. E. Stark, "Unified design of iterative receivers using factor graphs," *IEEE Trans. Inf. Theory*, vol. 47, pp. 843–849, Feb. 2001.

[27] U. Mengali and A. N. D'Andrea, *Synchronization Techniques for Digital Receivers (Applications of Communications Theory)*. Plenum Press, 1997.

[28] H. Meyr, M. Moeneclaey, and S. A. Fechtel, *Digital Communication Receivers*. John Wiley & Sons, 1998.

[29] P. Moqvist and T. Aulin, "Power and bandwidth efficient serially concatenated CPM with iterative decoding," in *Proc. IEEE Global Telecommun. Conf.* (San Francisco, CA), Dec. 2000.

[30] S. ten Brink and G. Kramer, "Design of repeat–accumulate codes for iterative detection and decoding," *IEEE Trans. Signal Processing*, vol. 51, pp. 2764–2772, Nov. 2003.
[31] M. Xiao and T. Aulin, "Irregular repeat continuous phase modulation," *IEEE Commun. Lett.*, vol. 9, pp. 723–725, Aug. 2005.
[32] S. Crozier and P. Guinand, "High-performance low-memory interleaver banks for turbo-codes," in *Proc. IEEE Vehicular Tech. Conf., VTC Fall 2001*, pp. 2394–2398, Oct. 2001.

Alan Barbieri was born in Parma, Italy, in 1979. He received the Dr. Ing. degree in Telecommunications Engineering (cum laude) and the Ph. D. degree in Information Technology from the University of Parma, Parma, Italy, in 2003 and 2007, respectively. Currently, he is a Research Associate at Dipartimento di Ingegneria dell'Informazione (DII), University of Parma.

His main research interests include digital transmission theory and information theory, with particular emphasis on channel coding, iterative joint detection and decoding algorithms, estimation of unknown parameters and algorithms for synchronization. He participates in several research projects funded by the European Space Agency (ESA-ESTEC) and important telecommunications companies.

Mr. Barbieri was the recipient of the Premio Conti for the year 2003, as the best graduate in Information Engineering at the University of Parma in the academic year 2003.

Giulio Colavolpe (S'96-M'00) was born in Cosenza, Italy, in 1969. He received the Dr. Ing. degree in Telecommunications Engineering (cum laude) from the University of Pisa, Italy, in 1994 and the Ph.D. degree in Information Technology from the University of Parma, Italy, in 1998. Since 1997, he has been at the University of Parma, Italy, where he is now an Associate Professor of Telecommunications. In 2000, he was Visiting Scientist at the Institut Eurécom, Valbonne, France.

His main research interests include digital transmission theory, adaptive signal processing, channel coding and information theory. His research activity has led to numerous scientific publications in leading international journals and conference proceedings and a few industrial patents. He is also co-author of the book *Detection Algorithms for Wireless Communications, with Applications to Wired and Storage Systems* (New York: John Wiley & Sons, 2004). In 2005, he received the best paper award at the 13th International Conference on Software, Telecommunications and Computer Networks (SoftCOM'05).